1521-009X/48/10/925–933$35.00
Drug Metabolism and Disposition
https://doi.org/10.1124/dmd.120.000075
Drug Metab Dispos 48:925–933, October 2020

Quantification of Neonatal Fc Receptor and Beta-2 Microglobulin in Human Liver Tissues by Ultraperformance Liquid Chromatography–Multiple Reaction Monitoring–based Targeted Quantitative Proteomics for Applications in Biotherapeutic Physiologically-based Pharmacokinetic Models [S]

Xiazi Qiu and Michael Zhuo Wang

Department of Pharmaceutical Chemistry, School of Pharmacy, University of Kansas, Lawrence, Kansas

Received April 11, 2020; accepted July 7, 2020

ABSTRACT

Neonatal Fc receptor (FcRn) and beta-2 microglobulin (β2M) play an important role in transporting maternal IgG to fetuses, maintaining the homeostasis of IgG and albumin in human body, and prolonging the half-life of IgG- or albumin-based biotherapeutics. Little is known about the influence of age, gender and race, and interindividual variability of human FcRn and β2M on the protein level. In this study, an ultraperformance liquid chromatography–multiple reaction monitoring mass spectrometry–based targeted quantitative proteomic method was developed and optimized for the quantification of human FcRn and β2M. Among the 39 human livers studied (age 13–80 years), the mean (±S.D.) concentrations of FcRn and β2M were 147 (±39) and 1250 (±460) pmol/g of liver tissue, respectively. A four-fold interindividual variability (63–243 pmol/g of liver tissue) was observed for the hepatic FcRn concentration. A moderate correlation was found between the hepatic β2M and FcRn expression levels. Influences of age, gender, and race on the hepatic expression of FcRn and β2M were evaluated. The findings from this study may aid the development of physiologically-based pharmacokinetic models that incorporate empirical FcRn tissue concentrations and interindividual variabilities, and the development of personalized dosing of biopharmaceuticals.

SIGNIFICANCE STATEMENT

This is the first study to evaluate the influence of age, gender, and race on the expression of neonatal Fc receptor (FcRn) and beta-2 microglobulin (β2M) and their interindividual variability in human livers. This study describes a validated ultraperformance liquid chromatography–multiple reaction monitoring–based targeted quantitative proteomic method for quantifying human FcRn and β2M in biological tissues. Results from this study may aid current development of physiologically-based pharmacokinetic models for biotherapeutics, where FcRn plays a significant role in clearance mechanism, and its expression level and interindividual variability are largely unknown.

Introduction

Human neonatal Fc receptor (FcRn) is a beta-2 microglobulin (β2M)–associated nonclassic major histocompatibility complex (MHC) class I family member (Blumberg et al., 1995; Roopenian and Akilesh, 2007; Kuo and Aveson, 2011; Pyzik et al., 2015, 2019), and it serves several essential roles during human development. This receptor is responsible for providing fetuses with maternal humoral immunity by passing antibodies from mothers to fetuses across placenta, and maintaining the homeostasis of endogenous IgG and albumin throughout the human life (Blumberg et al., 1995; Roopenian and Akilesh, 2007; Kuo and Aveson, 2011; Pyzik et al., 2015, 2017, 2019). These roles are achieved by binding the pinocytosed IgG or albumin to FcRn in the acidic endosomal compartment, then recycling the bound protein back to the cell surface, thus protecting IgG or albumin from lysosomal degradation (Roopenian and Akilesh, 2007; Pyzik et al., 2015; Fan and Neubert, 2016). This recycling mechanism provides a platform to engineer IgG- or albumin-based biopharmaceuticals, either to extend or shorten their half-lives. The protection from catabolism using FcRn recycling mechanism is a determining factor in the systemic pharmacokinetics (PK) of IgG- or albumin-based biotherapeutics, and plays an indispensable role in the biotherapeutic distribution to tissues at the site of action from systemic circulation (Wang and Zhou, 2016). Currently, most research has been focusing on using the binding affinity of monoclonal antibody–based biotherapeutics to FcRn to predict the drug's PK profiles (mainly systemic PK); however, the correlation between the in vivo PK profiles and such binding affinity still remains elusive (Datta-Mannan and Wroblewski, 2014).

To aid biotherapeutic drug development, physiologically-based pharmacokinetic (PBPK) modeling has been used to predict the half-life of

This work was supported in part by the National Institutes of Health and the *Eunice Kennedy Shriver* National Institute of Child Health and Human Development [Grant R03HD089006-01]. The content is solely the responsibility of the authors and does not necessarily represent the official views of the National Institutes of Health.
https://doi.org/10.1124/dmd.120.000075.
[S] This article has supplemental material available at dmd.aspetjournals.org.

ABBREVIATIONS: β2M, beta-2 microglobulin; CI, confidence interval; FcRn, neonatal Fc receptor; IFN, interferon; LC, liquid chromatography; MHC, major histocompatibility complex; MRM, multiple reaction monitoring; MS, mass spectrometry; PBPK, physiologically-based pharmacokinetic; PK, pharmacokinetics; PNS, post-nucleus supernatant; UPLC, ultra-performance liquid chromatography.

investigational biopharmaceuticals. Given the important role of FcRn in the distribution and clearance of IgG- or albumin-based biotherapeutics, FcRn tissue concentration is a necessary physiological parameter to be included in these models. In earlier models, the FcRn expression level usually relies on estimation (Shah and Betts, 2012; Hardiansyah and Ng, 2018), and is given a universal value for the whole model system. Recently, there has been a growing interest in determining tissue-specific biotherapeutic distribution and metabolism by incorporating site-specific PK in PBPK models (Wang and Zhou, 2016; Eigenmann et al., 2017). To achieve these site-specific PBPK models, tissue-specific FcRn concentration is required. A number of studies have tried to measure the FcRn expression level in various samples using antibody-based immunoquantification methods or real-time polymerase chain reaction (Israel et al., 1997; Martín et al., 1997; Haymann et al., 2000; Schlachetzki et al., 2002; Shah et al., 2003; Deane et al., 2005; Stirling et al., 2005; Akilesh et al., 2007; Cianga et al., 2007; Hornby et al., 2014; D'Hooghe et al., 2017; Latvala et al., 2017; Swiercz et al., 2017; Li and Balthasar, 2018; Lozano et al., 2018), which can suffer from cross-reactivity, low reproducibility, and/or poor mRNA-protein correlation. To overcome these limitations, we have previously developed ultraperformance liquid chromatography (UPLC)–multiple reaction monitoring (MRM)–based targeted quantitative proteomic methods to achieve absolute (as opposed to relative) quantification of drug-metabolizing enzymes and drug transporters (Wang et al., 2008; Michaels and Wang, 2014; Peng et al., 2015; Chen et al., 2016). Recently, a liquid chromatography (LC)/mass spectrometry (MS) quantification method for human FcRn in the transgenic Tg32 mouse line and in various human tissues from a limited number of donors ($n = 5$) was reported (Fan et al., 2016, 2019; Fan and Neubert, 2016). This method requires packing a column with antipeptide antibodies raised against selected tryptic peptides for peptide enrichment after sample digestion by trypsin. However, an antibody-free targeted quantitative proteomic method for FcRn has not yet been reported. As such, here we describe the development of a UPLC-MRM–based targeted quantitative proteomic method to quantify human FcRn and its binding partner β2M in human liver tissues, and evaluate their interindividual variability and effects of age, gender, and race on their expressions.

Materials and Methods

Chemicals and Reagents. Ammonium bicarbonate and dithiothreitol were obtained from Sigma-Aldrich (St. Louis, MO). Iodoacetamide, sodium deoxycholate, and sucrose were purchased from Sigma Life Science (St. Louis, MO). Optima-LC/MS grade water, acetonitrile, water with 0.1% (v/v) formic acid, and formic acid were bought from Fisher Scientific (Fair Lawn, NJ). Imidazole and phenylmethylsulfonyl fluoride were acquired from Acros Organics (Fair Lawn, NJ). EDTA was from Fluka Biochemika (Buchs, Switzerland). Anhydrous 2-propanol was obtained from Alfa Aesar (Ward Hill, MA). Bicinchoninic acid (BCA) assay and albumin standard were purchased from Thermo Scientific (Rockford, IL). Frozen sequencing grade modified trypsin was acquired from Promega (Madison, WI). Synthetic unlabeled AQUA™ peptides (light peptides; Ultimate grade) were manufactured by ThermoFisher Scientific, quantified as 5 pmol/μL (±5%–10%) by amino acid analysis with >97% purity measured by high-performance liquid chromatography UV (detection wavelength = 220 nm), and delivered as individual aliquoted solution in 5% acetonitrile in water. Synthetic ^{13}C and ^{15}N stable isotope–labeled crude signature peptides (heavy

TABLE 1

Signature peptides for FcRn and β2M, and their corresponding MRM methods

Protein	Signature Peptide[a]	Start to End[b]	Average Mass MH^{+}[c]	MRM		Cone	CE[e]
				Precursor Ion	Product Ion[d]		
			Da	m/z	m/z	V	eV
β2M	VNHVTLSQPK	102–111	1123.3	562.16	351.18	56	22
					455.26		18
					673.39		20
	VNHVTLSQP(K)		1131.3	566.06	351.18		22
					459.26		18
					681.39		20
	IQVYSR	27–32	765.9	383.45	425.21	32	16
					524.28		12
					652.34		14
	IQVYS(R)		775.9	388.42	435.26		16
					534.27		12
					662.34		14
FcRn	WQQQDK	164–169	832.9	416.95	500.25	34	16
					518.26		14
					629.29		16
	WQQQD(K)		840.9	420.95	508.25		16
					526.26		14
					637.29		16
	VELESPAK	288–295	873.0	437.00	315.20	32	20
					644.36		14
					773.40		16
	VELESPA(K)		881.0	440.97	323.20		20
					652.36		14
					781.40		16
	LFLEAFK	97–103	868.1	434.54	365.22	20	18
					607.35		12
					754.41		16
	LFLEA(F)K		878.1	439.54	375.22		18
					617.35		12
					764.41		16

[a]Stable isotope–labeled amino acid residues are included in parentheses.
[b]Start and end residue positions of peptides in the corresponding full-length protein.
[c]Theoretical average mass of monoprotonated molecular ion.
[d]Bolded product ions were used as the quantification trace.
[e]CE = collision energy

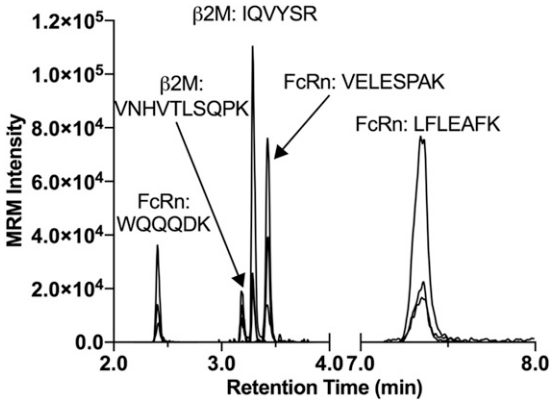

Fig. 1. UPLC-MRM chromatograms of FcRn and β2M heavy stable isotope–labeled signature peptides. Three transitions of each peptide were monitored, and the highest MS intensity was used as quantification trace in the analysis.

peptides) were also synthesized and delivered by ThermoFisher Scientific in 50% acetonitrile and 0.1% trifluoroacetic acid.

Human Liver Tissues. There were 39 single-donor human liver tissue samples used for this study, which included 31 livers from Caucasian donors, seven livers from African American donors, and one liver from a Hispanic donor (Supplemental Table 1). They were purchased from XenoTech (Kansas City, KS) or obtained from the University of Kansas Liver Center Tissue Bank (Kansas City, KS). These livers were obtained under protocols approved by respective committees at the source institutes for the conduct of human research. All liver tissues were stored at −80°C until sample preparation and analysis.

Post-nucleus Supernatant Preparation. Post-nucleus supernatant (PNS) was prepared for each liver tissue according to a previously published protocol (de Araújo et al., 2008, 2015). Briefly, a piece of liver tissue (19.6–250 mg) was homogenized in the homogenization buffer (10 μL per mg of liver), which consists of 250 mM sucrose, 3 mM imidazole, 1 mM EDTA, and 1 mM phenylmethylsulfonyl fluoride (pH 7.4), using a prechilled Dounce homogenizer (Radnoti LLC, Covina, CA). The homogenate was then centrifuged at 2000*g*, 4°C for 10 minutes. The resulted pellet (P1) was reconstituted with 50 μL PBS, and the supernatant was centrifuged again at 2000*g*, 4°C for 10 minutes. The second pellet (P2) was reconstituted in the same way as P1, and the supernatant was collected as PNS. Protein concentrations in PNS, P1, and P2 were determined using the BCA assay following the manufacturer's protocol.

Trypsin Digestion. To improve the solubility of FcRn and β2M during digestions, we followed a trypsin digestion protocol previously developed for hepatic transmembrane drug transporters (Peng et al., 2015). In short, 10 μg (unless stated otherwise) of each protein sample was denatured, solubilized, and reduced with dithiothreitol (4 mM final concentration) in 100 mM ammonium bicarbonate containing 10% (w/v) sodium deoxycholate at 56°C for 30 minutes. Then, samples were alkylated with iodoacetamide (10 mM final concentration) at dark for 20 minutes under room temperature. After alkylation, samples were diluted with 100 mM ammonium bicarbonate so that sodium deoxycholate concentration was reduced to 1% (w/v) during trypsin digestion. The trypsin digestion was initiated by adding 0.5 μg trypsin, and was carried out at 37°C for either 6 or 36 hours unless stated otherwise. All digestions were performed in Eppendorf Protein LoBind microcentrifuge tubes (Hamburg, Germany) to prevent adsorption of protein and peptides to the tube, and capped tubes were sealed with parafilm during incubation to reduce solvent evaporation during the digestion. Reactions (400 μL) were quenched with 200 μL quench solution that consisted of acetonitrile, a mixture of stable isotope–labeled signature peptides as internal standards (10 μL), and formic acid (0.67% v/v final concentration after quench). Quenched samples were incubated at room temperature for 20 minutes with gentle shaking to allow complete acid precipitation of sodium deoxycholate, followed by centrifugation at 16,000*g*, 4°C for 20 minutes. Supernatants (80% of total volume) was taken to a new Eppendorf Protein LoBind microcentrifuge tube, and evaporated to dryness using SpeedVac (Thermo Savant, Waltham, MA). Dried samples were store at −80°C until MS analysis. After equilibrating cold tubes to room temperature, dried samples were reconstituted with 150 μL 5% (v/v) acetonitrile and 0.5% (v/v) formic acid, incubated at room temperature for 20 minutes with gentle shaking, and centrifuged at 16,000*g*, 4°C for 20 minutes. Resulted supernatant was taken into a bovine serum albumin–passivated polypropylene vial (Agilent Technologies, Santa Clara, CA) (Chen et al., 2016) and loaded onto an autosampler (6°C). Trypsin digestion was further optimized by examining various digestion times (2, 4, 6, 16, 24, 36, and 48 hours) and different trypsin-to-protein ratios (1:5, 10, 20, 30, 40, 60, 80, and 100).

Signature Peptide Selection. Signature tryptic peptides were selected based on previous published criteria (Peng et al., 2015). Here we also avoided tryptic peptides beginning with or followed by acidic residues (i.e., aspartic and glutamic acids) due to their tendency to cause incomplete digestion by trypsin (Šlechtová et al., 2015). The specificity of each signature peptide was evaluated using the protein BLAST search against the nonredundant human protein sequences database (https://blast.ncbi.nlm.nih.gov).

Preparation of Calibration Standards. The absolute quantification of β2M and FcRn was achieved using synthetic light peptides as calibration standards. Calibration standards (ranging from 0.007 to 133 nM) were prepared with the addition of 10 μg blank CD-1 mouse plasma (lithium heparin; Innovative Research, Inc., Novi, MI) as the surrogate matrix using identical digestion protocol described above. A double blank standard (i.e., no surrogate matrix and no light peptides) and a blank standard (i.e., no light peptides) were also prepared

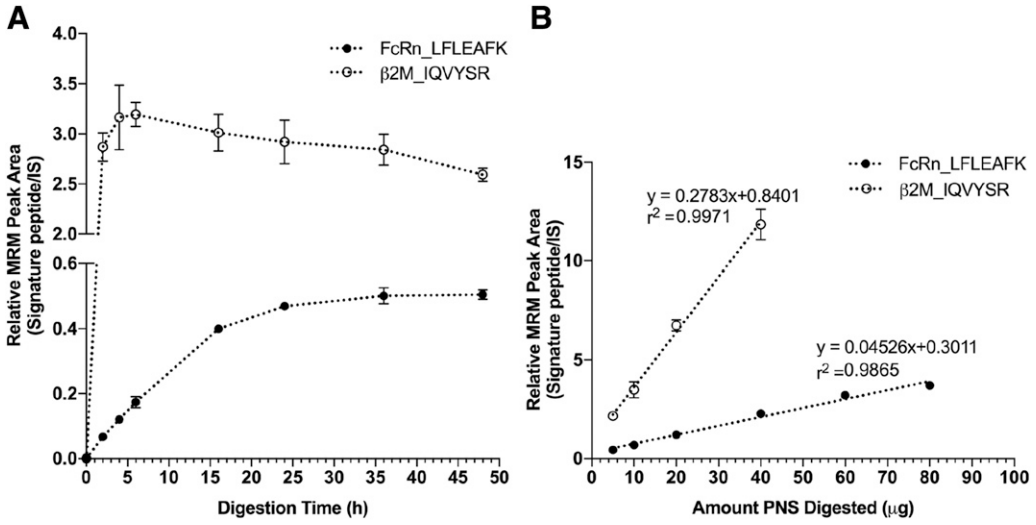

Fig. 2. Influences of trypsin digestion time (A) and trypsin:protein ratio (B) on the UPLC-MRM signals of both signature peptides. The relative MRM peak area was determined by normalizing light peptide area from PNS digest to the spiked-in isotope-labeled signature peptides. Symbols and error bars represent the average and S.D. of triplicate digestions, and the dotted lines in (B) denotes the best-fit lines determined using least-square linear regression analysis.

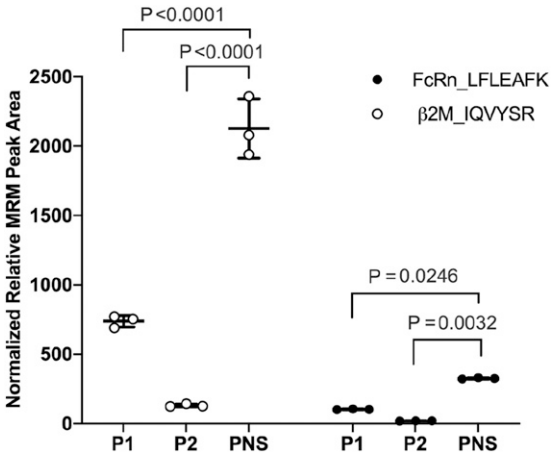

Fig. 3. Recovery of FcRn and β2M in isolated PNS. The normalized relative MRM peak area was determined by normalizing the ratio of light peptide area and the spiked-in heavy peptides area from 10 μg digest to the total amount of protein in isolated PNS. Lines and error bars represent the average and S.D. of triplicate digestions. Symbols represent the normalized relative MRM peak area from each of the triplicate digestion. Unpaired two-tailed *t* test was used to compare the values from P1, P2, and PNS. Quantitative recovery percentages are listed in Table 2.

to evaluate the background from digestion reagents and the surrogate matrix. No significant background was observed using blank CD-1 mouse plasma as the surrogate matrix in the LC–MRM analysis. Quality control samples were made separately in triplicates at 0.1, 1, 30, and 120 nM. Measurements from triplicates of each quality control concentration were used to calculate CVs for quantification of both peptides from UPLC-MRM analysis.

UPLC–Tandem MS Analysis. Digested samples were analyzed on a Waters Xevo TQ-S triple quadrupole mass spectrometer coupled with a Waters Acquity UPLC-I class system (Milford, MA). Each injection (10 μL) underwent reverse phase separations on a Waters UPLC BEH C18 analytical column (1.7 μm, 2.1 × 100 mm) with an attached in-line filter. The mobile phases were water with 0.1% (v/v) formic acid (A) and acetonitrile with 0.1% (v/v) formic acid (B). The LC gradient used was identical to previous study (Chen et al., 2016). The MRM methods were tuned and developed by infusing crude synthetic stable isotope–labeled peptides to the mass spectrometer along with an LC flowing at 0.2 ml/min and 50% B under positive electrospray ion mode. IntelliStart (Waters) was used to help guide the MRM development. The final MS tune setting used are as follows: capillary voltage = 1.50 kV; source offset = 50 V; desolvation temperature = 500 °C; desolvation gas = 1000 L/h; nebulizer gas = 7.0 bar. Specific optimized collision energy and cone voltage for each transition are listed in Table 1.

Data Analysis. The concentration of FcRn and β2M were calculated using TargetLynx (Waters). The mean value of three separate digestions were plotted for reported figures. Measured FcRn concentrations from 39 donors passed all four normality tests available (Anderson-Darling test, D'Agostino-Pearson test, Shapiro-Wilk test, and Kolmogorov-Smirnov test) (Supplemental Table 2). One measured β2M concentration (Donor L110D6) was determined to be an outlier using Grubb's test with alpha set to 0.05, and with the exclusion of the outlier, measured β2M concentrations also passed all four normality tests (Supplemental Table 2). Unpaired two-tailed *t* test was used to compare the normalized response ratio in the recovery experiment, expression levels between the female group and male groups, and concentrations between Caucasian and African American donors. Ordinary one-way ANOVA followed by Tukey's multiple comparisons test with a single pooled variance was used to evaluate the age influences on these two protein expression levels. Difference was considered significant if the *P* value was less than 0.05. Correlation analysis was performed by plotting measured β2M expression levels versus FcRn expression levels from the same sample for all 39 donors. Pearson *r* and *P* values were reported for the assessment of quality of the correlation. All data analyses were conducted in GraphPad Prism (version 7.03; San Diego, CA).

Results

Selection of Signature Peptides for FcRn and β2M. Based on the in silico selection criteria for signature peptides (Peng et al., 2015), three tryptic peptides were deemed suitable for targeted quantification of FcRn, and two for β2M (Table 1). The separation and detection of these signature peptides by the UPLC-MRM targeted quantitative proteomic method developed herein are demonstrated using their stable heavy isotope–labeled analogs (Fig. 1). For each peptide, three product ions were monitored in the MRM methods according to the recommendation of a recent white paper on applying quantitative proteomics in translational pharmacology research (Prasad et al., 2019). The transition gave the highest MS intensity was used as quantification trace in the analysis, and the other two transitions were used as confirmatory traces.

TABLE 2

Recovery percentage of FcRn and β2M in P1, P2, and PNS

	β2M	FcRn
	%	%
P1	24.7	23.0
P2	4.4	4.5
PNS	71.0	72.5

Optimization of Trypsin Digestion Time and Trypsin:Protein Ratio. To ensure a complete digestion, the effect of digestion duration was assessed using the PNS generated from one donor liver (L369D1; Supplemental Table 1). An aliquot (10 μg) of the PNS was digested for 2, 4, 6, 16, 24, 36, or 48 hours, and the relative LC-MRM signal over different digestion time is presented in Figure 2A. Due to the low expression of the target proteins, only one signature peptide (LFLEAFK) was detected and quantifiable for FcRn. Similarly, only one signature peptide (IQVYSR) was detected and quantified for β2M. The lack of detection for other signature peptides was likely due to their significantly lower signals and higher surrounding backgrounds as evidenced by actual chromatogram of the digestion of L369D1 PNS (Supplemental Fig. 1). The relative signal of IQVYSR of β2M reached maxima at 6 hours and gradually decreased thereafter. In contrast, LFLEAFK of FcRn did not reach the plateau until 36 hours. Therefore, 6 and 36 hours of trypsin digestion time were chosen for the subsequent β2M and FcRn quantification, respectively.

To assess the dynamic range of sample amount used in digestion, various quantity (5–100 μg) of PNS (from donor L369D1) was digested using 1 μg trypsin. β2M signature peptide, IQVYSR, showed a linear range from 5 to 40 μg protein loading ($r^2 > 0.99$), whereas FcRn

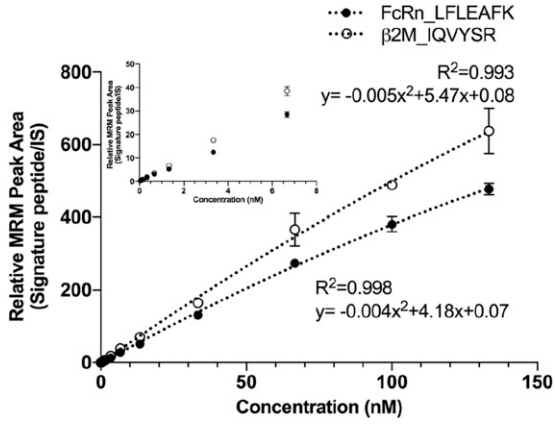

Fig. 4. Standard curves of FcRn and β2M quantification. The relative MRM peak area was determined by normalizing light peptide area to the spiked-in heavy peptides. Symbols and error bars represent the average and S.D. of triplicate injections of the same standard digest, and the dotted lines denotes the best-fit lines determined using quadratic fitting with 1/*x* weighting. The insert shows a blow-up of the lower standard concentration region.

TABLE 3

Summary of analytical performance of the UPLC-MRM method for FcRn and β2M signature peptides

Protein	Signature Peptide	LLOQ[a]	ULOQ[a]	Accuracy (CV)			
				0.1 nM QC[a]	1 nM QC	30 nM QC	120 nM QC
		nM	nM	%	%	%	%
β2M	IQVYSR	0.067	133.3	ND[a]	96 (4.5)	98 (7.2)	115 (10.6)
FcRn	LFLEAFK	0.007	133.3	86 (25.7)	83 (2.8)	90 (3.0)	100 (1.4)

[a]LLOQ, lower limit of quantification; ND, not determined; QC, quality control; ULOQ, upper limit of quantification.

signature peptide, LFLEAFK, exhibited linearity from 5 to 80 μg ($r^2 >$ 0.98) (Fig. 2B). The shortened linearity range for β2M protein loading was due to an interfering peak observed in internal standard transitions for IQVYSR starting from 60 μg PNS loading (data not shown). Therefore, to minimize interference of the β2M heavy peptide, 10 μg protein loading was chosen for the subsequent analysis.

Target Protein Recovery in PNS Preparation and Scaling Factor Determination. P1 and P2 of the donor (L369D1) were reconstituted in 50 μL PBS, and a 10 μg aliquot of P1, P2, and PNS was digested to investigate recoveries of FcRn and β2M from PNS isolation. Both FcRn and β2M response ratio (normalized to total protein) were found to be significantly different from P1 and P2 (Fig. 3). The recovery percentage was calculated based on the normalized total protein response ratio. β2M and FcRn had a 71.0% and 72.5% recovery, respectively (Table 2). To determine the scaling factor, the total PNS protein concentration was determined for all 39 donor livers and it averaged 87 μg per mg liver tissue (S.D. = 19 μg), and the average volume of PNS isolated according to our protocol was 8.1 μL per mg liver tissue (S.D. = 0.64 μL).

Absolute Quantification of FcRn and β2M in Human Livers. Absolute quantification of FcRn and β2M were calculated from standard curves of light peptides of their respective signature peptides (Fig. 4; Supplemental Fig. 2). Quality control samples were prepared to evaluate the performance of the method, which was summarized in Table 3.

FcRn and β2M concentrations were determined in PNS isolated from a total of 39 human livers and normalized to per gram of liver tissue using the established scaling factor and target protein recovery percentages determined above (Fig. 5). Overall, mean FcRn concentration [mean with 95% confidence interval (CI)] was found to be 147.0 (134.3–159.7) pmol/g liver tissues and mean β2M concentration (mean with 95% CI) was found to be 1248 (1099–1397) pmol/g liver tissues.

Gender Influence on FcRn and β2M Expression in Human Livers. The gender influences on FcRn and β2M expression in human livers are shown in Figure 6. There were no significant differences found in FcRn and β2M expression between the female group and male group. The female group had an average of 1243 (963.2–1522) and 139.5 (122.7–156.3) pmol/g liver tissues (mean with 95% CI) of β2M and FcRn, respectively, whereas the male group had an mean value of 1253 (1102–1404) and 154.1 (134.3–173.9) pmol/g liver tissues (mean with 95% CI) of β2M and FcRn, respectively.

Age Influence on FcRn and β2M Expression in Human Livers. To investigate the age influences on FcRn and β2M expression in human livers, donors were grouped into six age group bins (<20, 21–30, 31–40, 41–50, 51–60, and >61; Fig. 7). There were no statistical significances found among different age groups using one-way ANOVA. A summary of average concentration and 95% CI is reported in Table 4.

Race Influence on FcRn and β2M Expression in Human Livers. There were thirty-one Caucasian donors, seven African American donors, and one Hispanic donor of unknown race. The measured hepatic FcRn and β2M expression levels were compared to assess differences between Caucasians and African Americans (Fig. 8; Supplemental Fig. 3). For FcRn, there was no statistically significant difference between the two races. In contrast, a significant difference was found for the β2M expression between the two races ($P = 0.0218$). However, after removing the statistical outlier β2M expression value from Donor L110D6 (African American; see *Data Analysis* under *Materials and Methods* and Supplemental Fig. 2D), the difference became insignificant ($P = 0.2815$; Supplemental Fig. 3). Regardless, caution should be taken when interpreting these results due to the limited number of African American donor livers ($n = 7$) available in this study.

Correlation between FcRn and β2M Expression Levels in Human Livers. FcRn expression levels were correlated with β2M expression levels in human livers for all donors. There is a moderate positive correlation found between these two values among the 39 donors (Fig. 9; $r = 0.4739$, $P = 0.0023$). A better correlation can be achieved after removing the statistical outlier β2M expression value from Donor L110D6 (Supplemental Fig. 4; $r = 0.5668$, $P = 0.0002$). Overall, one can expect a higher concentration of FcRn in the liver if it was found that there is a high liver concentration of β2M.

Discussion

Determination of human hepatic FcRn expression and its interindividual variability will help the development of PBPK models to understand the distribution and clearance of IgG- or albumin-based biopharmaceuticals, especially models that include tissue-specific PK, as the current model lacks experimentally determined FcRn concentration. Hepatic FcRn has been found to play an important role in regulating albumin homeostasis, and to increase the susceptibility of acetaminophen-induced liver injury (Pyzik et al., 2017; Ward and Ober, 2017). Anti-FcRn pharmaceuticals have already been studied in clinical settings to evaluate its potential in blocking FcRn-IgG interaction to reduce symptoms caused by pathogenic IgG in autoimmune diseases

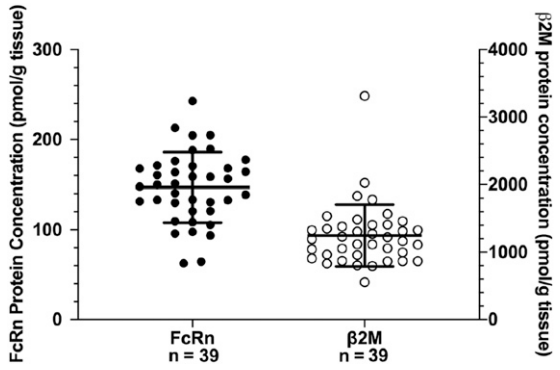

Fig. 5. Absolute quantification of FcRn and β2M in individual human livers (n = 39). Concentration of both proteins are expressed in picomole protein per gram of liver tissue. Lines and error bars represent the average and S.D. of all human liver analyzed. Symbols represent the average concentration determined from three separate digestions for each individual donor. The y-axis for FcRn quantification is plotted on the left, and the y-axis for β2M is plotted on the right.

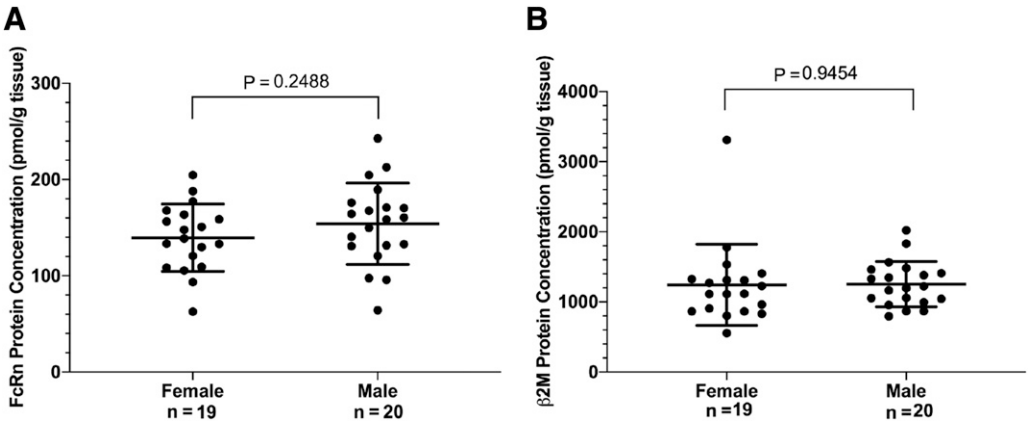

Fig. 6. FcRn (A) and β2M (B) concentrations based on gender. Lines and error bars represent the average and S.D. of all human liver analyzed in each gender group. Symbols represent the average concentration determined from three separate digestions for each individual donor. Unpaired two-tailed *t* test found no significant statistical differences between two groups for both FcRn and β2M.

(Ling et al., 2019). Therefore, understanding of age, gender, and race influence on human hepatic FcRn expression is of importance. In this study, a UPLC-MRM–based targeted proteomic quantification method was developed for human FcRn and β2M. Using this developed method, the influence of age, gender, and race on human hepatic FcRn and β2M expression levels was studied for the first time. This method allowed robust quantifications of FcRn and β2M in human liver tissues, which averaged (±S.D.) at 147.0 (±39) and 1248 (±460) pmol/g liver tissues respectively. The measured concentration of human hepatic FcRn was moderately higher than the measurements previously reported by Fan et al. (average ± S.D. 89.5 ± 42.3 pmol/g liver tissue, range 37.0–145.2 pmol/g liver tissue) (Fan et al., 2019), and is also higher than the human FcRn expression level found in the transgenic Tg32 mouse liver (average ± S.D. 55.38 ± 18.55 pmol/g liver tissue) (Fan et al., 2016; Fan and Neubert, 2016). The major differences between our FcRn quantification method and Fan's method include the sample enrichment (antibody-free PNS vs. antipeptide immunocapture), the length of digestion time (36 hours vs. 16 hours), the digestion method (in-solution

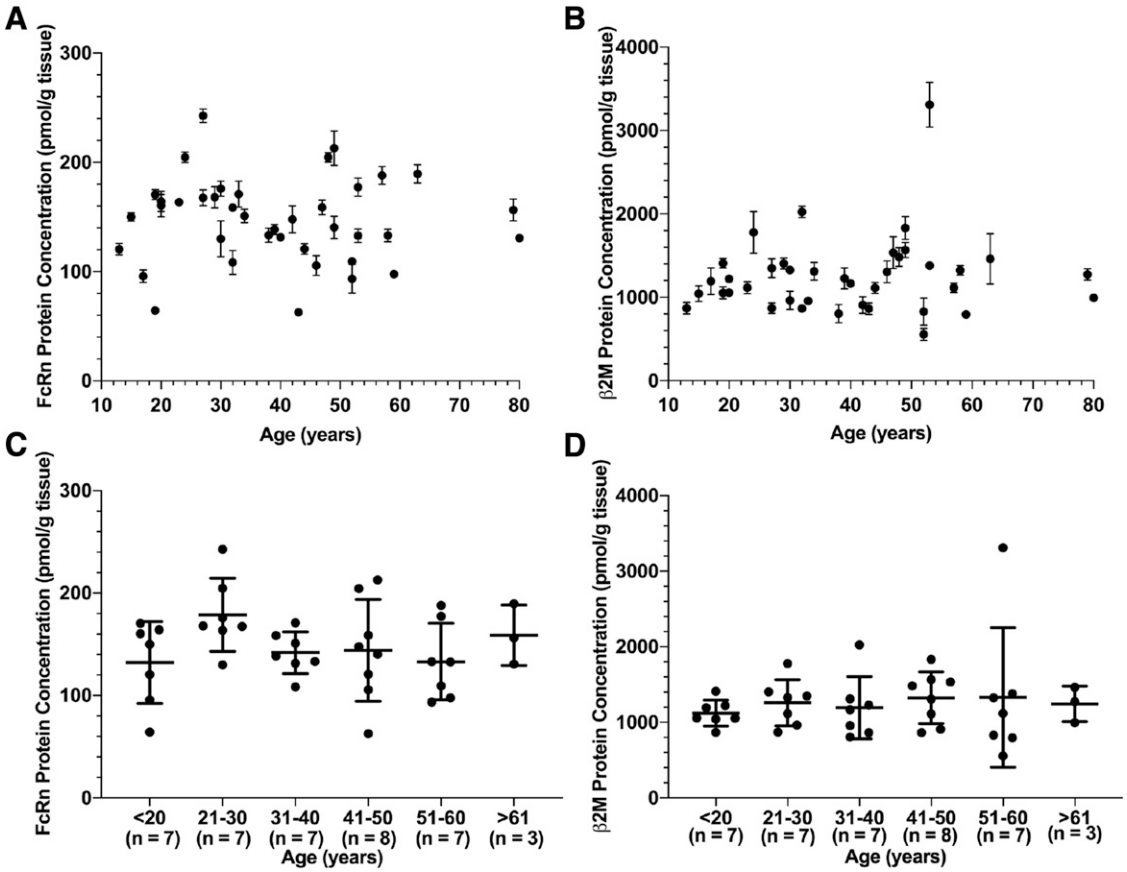

Fig. 7. FcRn (A and C) and β2M (B and D) concentrations based on age. (A and B) Symbols and error bars represent the average and S.D. of triplicates of digestion for each human liver donor. (C and D) Lines and error bars represent the average and S.D. of all human liver analyzed in each age group. Symbols represent the average concentration determined from three separate digestions for each individual donor. One-way ANOVA followed by Tukey's multiple comparisons test with a single pooled variance found no significant statistical differences among age groups for both FcRn and β2M.

TABLE 4

Summary of average concentration and 95% CI of FcRn and β2M for different age groups

Protein	Concentration (pmol/g liver tissues)	Age groups (years)					
		<20	21–30	31–40	41–50	51–60	>61
β2M	Mean	1122	1258	1194	1326	1330	1244
	Lower 95% CI of mean	962.7	975.0	813.1	1040	476.8	662.1
	Upper 95% CI of mean	1281	1542	1576	1611	2184	1825
FcRn	Mean	132.3	178.9	141.8	144.2	133.1	158.9
	Lower 95% CI of mean	95.16	145.9	122.8	102.6	98.59	85.89
	Upper 95% CI of mean	169.4	211.9	160.7	185.8	167.7	231.9

vs. on-pellet), and the instrument used (triple quadrupole MS under MRM mode vs. quadrupole orbitrap MS under targeted selected ion monitoring mode). The difference between measurements from the two studies may be due to the variations caused by using light peptides as calibration standards other than recombinant proteins (Wang et al., 2008; Chen et al., 2016), though the method used in this study was carefully validated considering trypsin digestion efficiency. The discrepancy may be also due to the difference in the sample size as the number of donor livers used in our study ($n = 39$) is almost eight times larger than the one ($n = 5$) used in the previous study.

FcRn signature tryptic peptide, LFLEAFK, demonstrated a wider dynamic range in PNS total protein loading than β2M signature peptide, IQVYSR. This is due to an interference observed near the elution time in the quantification transition of the heavy-labeled peptide of IQVYSR. This interference was not significant until the protein loading was greater than 40 μg. If a large amount of PNS protein need to be digested for a future study, a potential solution for this interference is to use an internal standard that labels two amino acids with stable isotopes instead of one.

PNS was selected as the sample form for the analysis for the following reason. PNS eliminates the present nucleus in the sample, which was expected to reduce the potential interferences and signal suppression coming from nuclear proteins (e.g., histones), genomic DNAs, and RNAs. D'Hooghe et al. (2017) showed that FcRn was mainly localized in the endosomal compartment, and little was found in nucleus. Our recovery data suggest a minimal-to-moderate distribution of FcRn (as well as β2M) in the nucleus pellets (Table 2). The incomplete recovery of both proteins might be due to the choice of the homogenization buffer being non–detergent based, which is not ideal to fully solubilize membrane-bound proteins. The incorporation of an anionic detergent, sodium deoxycholate, in the digestion process is expected to achieve a more complete solubilization of membrane-bound FcRn and its binding partner β2M recovered in the PNS (Peng et al., 2015). The reason to choose a non–detergent based homogenization buffer was due to the goal of preserving intact organelles derived or isolated from the liver tissue for future intracellular distribution studies.

The measured human hepatic FcRn and β2M concentrations were evaluated between genders, among different age groups, and between Caucasian and African American donors. One of the limitations of this study is that the minimum age of liver donor was 13 years old, and neonatal and fetal livers were not included in this study. Although this study did not show a significant trend in the FcRn concentration in the age groups studied (age 13–80 years), previous studies have estimated FcRn expression levels in pediatric group using a minimal PBPK model (Hardiansyah and Ng, 2018). They estimated that as human development progresses, there is a decrease in FcRn concentration. (Martín et al., 1997) studied the intestine FcRn mRNA level throughout rat development, and found that it had the maximum mRNA level during 1–19 days of age, and was significantly lower during fetal and after weaning stages (). Hence, quantification of FcRn protein levels in fetal, neonatal, and young pediatric (<13 years old) donors using the developed targeted proteomic method is warranted to provide a complete picture of FcRn ontogeny in humans.

Even though there were no significant differences found among different age or gender groups, a nearly 4-fold interindividual variability for the hepatic FcRn expression was observed (range 63–243 pmol/g liver tissue, $n = 39$). Fan et al. also found the similar variability (3.9-fold, range 37.0–145.2 pmol/g liver tissue) in a very limited number of donor livers ($n = 5$) (Fan et al., 2019). These suggest other factors than age and gender influencing the hepatic FcRn expression. One potential factor is genetic polymorphism. Passot et al. listed two genetic polymorphisms of FcRn gene and indicated that one of them, a variable number tandem repeat at the promoter region, may influence the promoter activity, and result in differential expression of FcRn in humans (Passot et al., 2013).

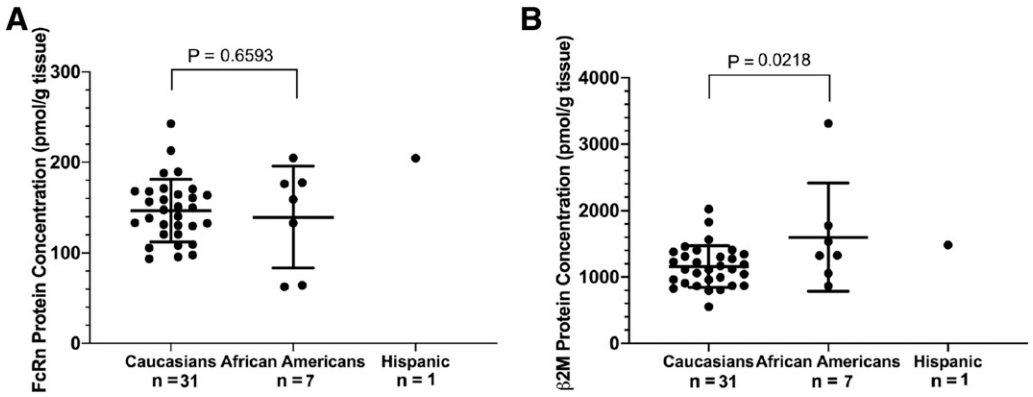

Fig. 8. FcRn (A) and β2M (B) concentrations based on race. Lines and error bars represent the average and S.D. of all human liver analyzed in each race group. Symbols represent the average concentration determined from three separate digestions for each individual donor. Unpaired two-tailed *t* test found no significant statistical differences between Caucasian and African American donors for FcRn expressions and found significant statistical differences ($P = 0.0218$) for β2M expressions including the statistical outlier determined by Grubb's test.

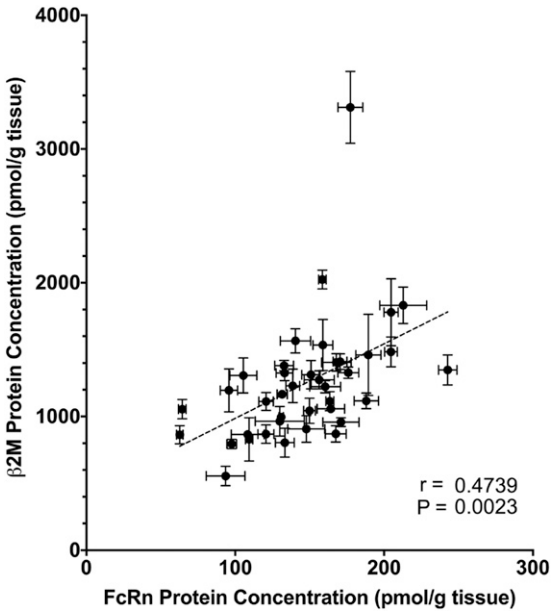

Fig. 9. Correlation analysis of FcRn concentration and β2M concentration (n = 39). Symbols and error bars represent the average and S.D. of triplicates of digestion for each human liver donor. The dotted line represents the best-fit lines determined using least-square linear regression analysis.

Further study on the influence of genetic variability on the FcRn expression is of importance to fully understand the underlying reason for the observed interindividual variability.

Human hepatic β2M displayed relative stable expression level throughout the age groups studied and between the female and male groups. One female donor (Donor L110D6, age 53, African American) exhibited significantly greater β2M concentration compared with other donors (Figs. 5 and 7B). Vraetz et al. (1999) found that after interferon (IFN)-α or -γ stimulant, there was a significant increase in β2M gene expression, protein synthesis, and protein secretion in HepG2, HuH7 human hepatoma cells, and other cell lines. Frost et al. (2011) discovered that human hepatocellular carcinoma and its adjacent liver tissues exhibited higher β2M mRNA expression levels than in the healthy liver tissue. Although the specific reason is unknown, it may be speculated that the donor may have been treated by IFN-γ or IFN-α prior to liver donation or that this tissue was adjacent to an unrecognized cancerous tissue.

In this study, it was found that β2M concentrations moderately correlated with FcRn concentrations in the liver (Fig. 9). β2M is a universal binding partner for all MHC class I molecules, plays an essential role in the surface expression of FcRn, and facilitates the binding between FcRn and IgG (Li et al., 2016). FcRn, as an MHC class I member homolog, exists as a homodimer while in the ER, and is more susceptible to endoglycosidase digestion when β2M is not present (Zhu et al., 2002). Mutation of β2M gene in humans leads to a rare disease called familial hypercatabolic hypoproteinemia, which presents as a lack of FcRn and a decreased level of circulating IgG and albumin (Wani et al., 2006; Ardeniz et al., 2015; Pyzik et al., 2019). Praetor and Hunziker (2002) demonstrated that without the presence of β2M, FcRn remained inside of the cell, and the binding between FcRn and IgG significantly decreased. These authors also speculated that the functional FcRn expression level might be regulated by the mRNA level of β2M in a tissue, species, and development stage dependent manner (Praetor and Hunziker, 2002). Our protein expression data appear to support this hypothesis.

In summary, a UPLC-MRM–based targeted quantitative proteomic method was developed for human FcRn and β2M. This method enabled the first study to probe age, gender, and race influence on FcRn and β2M expression in the human liver. Both FcRn and β2M expression levels exhibited independency regarding to age (13–80 years), gender, and race (Caucasian vs. African American), although a four-fold interindividual variability was found in the hepatic FcRn concentration. These results are expected to aid the development of IgG- and albumin-based biopharmaceuticals in terms of refining PBPK models and establishing personalized medicine.

Acknowledgments

We would like to acknowledge the University of Kansas Liver Center Tissue Bank (Kansas City, KS) for providing donor livers. We also thank Dr. Naitee Ting (Boehringer Ingelheim Pharmaceuticals, Inc.) for helpful discussions on statistical analysis.

Authorship Contributions

Participated in research design: Qiu, Wang.
Conducted experiments: Qiu.
Performed data analysis: Qiu, Wang.
Wrote or contributed to the writing of the manuscript: Qiu, Wang.

References

Akilesh S, Christianson GJ, Roopenian DC, and Shaw AS (2007) Neonatal FcR expression in bone marrow-derived cells functions to protect serum IgG from catabolism. *J Immunol* **179**: 4580–4588.
Ardeniz Ö, Unger S, Onay H, Ammann S, Keck C, Cianga C, Gerçeker B, Martin B, Fuchs I, Salzer U, et al. (2015) β2-Microglobulin deficiency causes a complex immunodeficiency of the innate and adaptive immune system. *J Allergy Clin Immunol* **136**:392–401.
Blumberg RS, Koss T, Story CM, Barisani D, Polischuk J, Lipin A, Pablo L, Green R, and Simister NE (1995) A major histocompatibility complex class I-related Fc receptor for IgG on rat hepatocytes. *J Clin Invest* **95**:2397–2402.
Chen Y, Zane NR, Thakker DR, and Wang MZ (2016) Quantification of flavin-containing monooxygenases 1, 3, and 5 in human liver microsomes by UPLC-MRM-based targeted quantitative proteomics and its application to the study of ontogeny. *Drug Metab Dispos* **44**:975–983.
Cianga P, Cianga C, Plamadeala P, Branisteanu D, and Carasevici E (2007) The neonatal Fc receptor (FcRn) expression in the human skin. *Virchows Arch* **451**:859–860.
Datta-Mannan A and Wroblewski VJ (2014) Application of FcRn binding assays to guide mAb development. *Drug Metab Dispos* **42**:1867–1872.
Deane R, Sagare A, Hamm K, Parisi M, LaRue B, Guo H, Wu Z, Holtzman DM, and Zlokovic BV (2005) IgG-assisted age-dependent clearance of Alzheimer's amyloid beta peptide by the blood-brain barrier neonatal Fc receptor. *J Neurosci* **25**:11495–11503.
de Araújo MEG, Huber LA, and Stasyk T (2008) in *Isolation of Endocitic Organelles by Density Gradient Centrifugation, in: 2D PAGE: Sample Preparation and Fractionation* (Posch A 317–331, Humana Press, Totowa, NJ.
de Araújo MEG, Lamberti G, and Huber LA (2015) Homogenization of mammalian cells. *Cold Spring Harb Protoc* **2015**:1009–1012.
D'Hooghe L, Chalmers AD, Heywood S, and Whitley P (2017) Cell surface dynamics and cellular distribution of endogenous FcRn. *PLoS One* **12**:e0182695.
Eigenmann MJ, Fronton L, Grimm HP, Otteneder MB, and Krippendorff BF (2017) Quantification of IgG monoclonal antibody clearance in tissues. *MAbs* **9**:1007–1015.
Fan Y-Y, Avery LB, Wang M, O'Hara DM, Leung S, and Neubert H (2016) Tissue expression profile of human neonatal Fc receptor (FcRn) in Tg32 transgenic mice. *MAbs* **8**: 848–853.
Fan YY, Farrokhi V, Caiazzo T, Wang M, O'Hara DM, and Neubert H (2019) Human FcRn tissue expression profile and half-life in PBMCs. *Biomolecules* **9**:373.
Fan Y-Y and Neubert H (2016) Quantitative analysis of human neonatal Fc receptor (FcRn) tissue expression in transgenic mice by online peptide immuno-affinity LC-HRMS. *Anal Chem* **88**: 4239–4247.
Frost K, Seir K, Lackner A, Grusch M, Grasl-Kraupp B, Schulte-Hermann R, and Rodgarkia-Dara C (2011) Inhibin/activin expression in human and rodent liver: subunits α and βB as new players in human hepatocellular carcinoma? *Br J Cancer* **104**:1303–1312.
Hardiansyah D and Ng CM (2018) Effects of the FcRn developmental pharmacology on the pharmacokinetics of therapeutic monoclonal IgG antibody in pediatric subjects using minimal physiologically-based pharmacokinetic modelling. *MAbs* **10**:1144–1156.
Haymann JP, Levraud JP, Bouet S, Kappes V, Hagège J, Nguyen G, Xu Y, Rondeau E, and Sraer JD (2000) Characterization and localization of the neonatal Fc receptor in adult human kidney. *J Am Soc Nephrol* **11**:632–639.
Hornby PJ, Cooper PR, Kliwinski C, Ragwan E, Mabus JR, Harman B, Thompson S, Kauffman AL, Yan Z, Tam SH, et al. (2014) Human and non-human primate intestinal FcRn expression and immunoglobulin G transcytosis. *Pharm Res* **31**:908–922.
Israel EJ, Taylor S, Wu Z, Mizoguchi E, Blumberg RS, Bhan A, and Simister NE (1997) Expression of the neonatal Fc receptor, FcRn, on human intestinal epithelial cells. *Immunology* **92**:69–74.
Kuo TT and Aveson VG (2011) Neonatal Fc receptor and IgG-based therapeutics. *MAbs* **3**: 422–430.
Latvala S, Jacobsen B, Otteneder MB, Herrmann A, and Kronenberg S (2017) Distribution of FcRn across species and tissues. *J Histochem Cytochem* **65**:321–333.
Li L, Dong M, and Wang XG (2016) The implication and significance of beta 2 microglobulin: a conservative multifunctional regulator. *Chin Med J (Engl)* **129**:448–455.

Li T and Balthasar JP (2018) FcRn expression in wildtype mice, transgenic mice, and in human tissues. *Biomolecules* **8**:115.
Ling LE, Hillson JL, Tiessen RG, Bosje T, van Iersel MP, Nix DJ, Markowitz L, Cilfone NA, Duffner J, Streisand JB, et al. (2019) M281, an anti-FcRn antibody: pharmacodynamics, pharmacokinetics, and safety across the full range of IgG reduction in a first-in-human study. *Clin Pharmacol Ther* **105**:1031–1039.
Lozano NA, Lozano A, Marini V, Saranz RJ, Blumberg RS, Baker K, Agresta MF, and Ponzio MF (2018) Expression of FcRn receptor in placental tissue and its relationship with IgG levels in term and preterm newborns. *Am J Reprod Immunol* **80**:e12972.
Martín MG, Wu SV, and Walsh JH (1997) Ontogenetic development and distribution of antibody transport and Fc receptor mRNA expression in rat intestine. *Dig Dis Sci* **42**: 1062–1069.
Michaels S and Wang MZ (2014) The revised human liver cytochrome P450 "Pie": absolute protein quantification of CYP4F and CYP3A enzymes using targeted quantitative proteomics. *Drug Metab Dispos* **42**:1241–1251.
Passot C, Azzopardi N, Renault S, Baroukh N, Arnoult C, Ohresser M, Boisdron-Celle M, Gamelin E, Watier H, Paintaud G, et al. (2013) Influence of FCGRT gene polymorphisms on pharmacokinetics of therapeutic antibodies. *MAbs* **5**:614–619.
Peng KW, Bacon J, Zheng M, Guo Y, and Wang MZ (2015) Ethnic variability in the expression of hepatic drug transporters: absolute quantification by an optimized targeted quantitative proteomic approach. *Drug Metab Dispos* **43**:1045–1055.
Praetor A and Hunziker W (2002) β(2)-Microglobulin is important for cell surface expression and pH-dependent IgG binding of human FcRn. *J Cell Sci* **115**:2389–2397.
Prasad B, Achour B, Artursson P, Hop CECA, Lai Y, Smith PC, Barber J, Wisniewski JR, Spellman D, Uchida Y, et al. (2019) Toward a consensus on applying quantitative liquid chromatography-tandem mass spectrometry proteomics in translational pharmacology research: a white paper. *Clin Pharmacol Ther* **106**:525–543.
Pyzik M, Rath T, Kuo TT, Win S, Baker K, Hubbard JJ, Grenha R, Gandhi A, Krämer TD, Mezo AR, et al. (2017) Hepatic FcRn regulates albumin homeostasis and susceptibility to liver injury. *Proc Natl Acad Sci USA* **114**:E2862–E2871.
Pyzik M, Rath T, Lencer WI, Baker K, and Blumberg RS (2015) FcRn: the architect behind the immune and nonimmune functions of IgG and albumin. *J Immunol* **194**:4595–4603.
Pyzik M, Sand KMK, Hubbard JJ, Andersen JT, Sandlie I, and Blumberg RS (2019) The neonatal Fc receptor (FcRn): a misnomer? *Front Immunol* **10**:1540.
Roopenian DC and Akilesh S (2007) FcRn: the neonatal Fc receptor comes of age. *Nat Rev Immunol* **7**:715–725.
Schlachetzki F, Zhu C, and Pardridge WM (2002) Expression of the neonatal Fc receptor (FcRn) at the blood-brain barrier. *J Neurochem* **81**:203–206.
Shah DK and Betts AM (2012) Towards a platform PBPK model to characterize the plasma and tissue disposition of monoclonal antibodies in preclinical species and human. *J Pharmacokinet Pharmacodyn* **39**:67–86.
Shah U, Dickinson BL, Blumberg RS, Simister NE, Lencer WI, and Walker WA (2003) Distribution of the IgG Fc receptor, FcRn, in the human fetal intestine. *Pediatr Res* **53**:295–301.
Šlechtová T, Gilar M, Kalíková K, and Tesařová E (2015) Insight into trypsin miscleavage: comparison of kinetic constants of problematic peptide sequences. *Anal Chem* **87**:7636–7643.
Stirling CM, Charleston B, Takamatsu H, Claypool S, Lencer W, Blumberg RS, and Wileman TE (2005) Characterization of the porcine neonatal Fc receptor--potential use for trans-epithelial protein delivery. *Immunology* **114**:542–553.
Swiercz R, Mo M, Khare P, Schneider Z, Ober RJ, and Ward ES (2017) Loss of expression of the recycling receptor, FcRn, promotes tumor cell growth by increasing albumin consumption. *Oncotarget* **8**:3528–3541.
Vraetz T, Ittel TH, van Mackelenbergh MG, Heinrich PC, Sieberth HG, and Graeve L (1999) Regulation of beta2-microglobulin expression in different human cell lines by proinflammatory cytokines. *Nephrol Dial Transplant* **14**:2137–2143.
Wang MZ, Wu JQ, Dennison JB, Bridges AS, Hall SD, Kornbluth S, Tidwell RR, Smith PC, Voyksner RD, Paine MF, et al. (2008) A gel-free MS-based quantitative proteomic approach accurately measures cytochrome P450 protein concentrations in human liver microsomes. *Proteomics* **8**:4186–4196.
Wang W and Zhou H (2016) Pharmacological considerations for predicting PK/PD at the site of action for therapeutic proteins. *Drug Discov Today Technol* **21–22**:35–39.
Wani MA, Haynes LD, Kim J, Bronson CL, Chaudhury C, Mohanty S, Waldmann TA, Robinson JM, and Anderson CL (2006) Familial hypercatabolic hypoproteinemia caused by deficiency of the neonatal Fc receptor, FcRn, due to a mutant beta2-microglobulin gene. *Proc Natl Acad Sci USA* **103**:5084–5089.
Ward ES and Ober RJ (2017) Hepatic function of FcRn revealed: implications for overcoming drug-mediated hepatotoxicity. *Hepatology* **66**:2083–2085.
Zhu X, Peng J, Raychowdhury R, Nakajima A, Lencer WI, and Blumberg RS (2002) The heavy chain of neonatal Fc receptor for IgG is sequestered in endoplasmic reticulum by forming oligomers in the absence of beta2-microglobulin association. *Biochem J* **367**:703–714.

Address correspondence to: Dr. Michael Zhuo Wang, Department of Pharmaceutical Chemistry, School of Pharmacy, The University of Kansas, 2095 Constant Ave., 252 Simons Labs, Lawrence, KS 66047. E-mail: michael.wang@ku.edu

Supplemental Data

Quantification of Neonatal Fc Receptor (FcRn) and Beta-2 Microglobulin (β2M) in Human Liver Tissues by UPLC-MRM-Based Targeted Quantitative Proteomics for Applications in Biotherapeutic PBPK Models

Xiazi Qiu and Michael Zhuo Wang

Department of Pharmaceutical Chemistry, School of Pharmacy, University of Kansas, Lawrence, Kansas (XQ and MZW)

Journal Title:

Drug Metabolism and Disposition

Supplemental Table 1. Summary of human liver donor information (n = 39).

University of Kansas Medical Center Liver Bank

KULTBID	Tube	Procedure Type	Pathological DX	Pathological Comments	Age	Sex	Race
L398D	1	Transplant-Donor	No diagnostic abnormalities	Stroke (Intracranial hemorrhage)	23	F	Caucasian
L914D	1	Transplant-Donor	No diagnostic abnormalities	Anoxia (Cardiovascular)	29	F	Caucasian
L1017D	1	Transplant-Donor	No diagnostic abnormalities	Anoxia (Cardiovascular); Post-perfusion biopsy	30	F	Caucasian
L844D	2	Transplant-Donor	No diagnostic abnormalities	Head Trauma	32	F	Caucasian
L1021D	1	Transplant-Donor	No diagnostic abnormalities	Head Trauma (GSW-Homicide)	34	F	Caucasian
L1019D	1	Transplant-Donor	No diagnostic abnormalities	Anoxia (Stroke); Post-perfusion biopsy	38	F	Caucasian
L1034D	1	Transplant-Donor	No diagnostic abnormalities	Stroke (Intracranial Hemorrhage)	39	F	Caucasian
L629D	1	Transplant-Donor	No diagnostic abnormalities	Stroke (Intracranial hemorrhage)	43	F	African-American
L789D	1	Transplant-Donor	No diagnostic abnormalities	Stroke (Head Bleed); Pre-perfusion biopsy	44	F	Caucasian
L424D	1	Transplant-Donor	No diagnostic abnormalities	Anoxia (Cardiovascular)	52	F	Caucasian
L110D	6	Transplant-Donor	No diagnostic abnormalities	Stroke (Intracranial hemorrhage)	53	F	African-American
L326D	1	Transplant-Donor	No diagnostic abnormalities	Anoxia (Cardiovascular)	79	F	Caucasian
L710D	1	Transplant-Donor	No diagnostic abnormalities	Asphyxia	13	M	Caucasian
L1128D	1	Transplant-Donor	No diagnostic abnormalities	Head Trauma (Blunt Injury- MVA)	15	M	Caucasian

L669D	1	Transplant-Donor	No diagnostic abnormalities	Head Trauma (Blunt injury, MVA)	17	M	Caucasian
L356DII		Transplant-Donor	No diagnostic abnormalities	Gunshot wound (Head)	19	M	African-American
L613D	1	Transplant-Donor	No diagnostic abnormalities	Stroke (Intracranial hemorrhage)	19	M	Caucasian
L244D	1	Transplant-Donor	No diagnostic abnormalities	Head trauma (Blunt injury)	20	M	Caucasian
L465D	1	Transplant-Donor	No diagnostic abnormalities	Gunshot wound (Head)	27	M	Caucasian
L369D	1	Transplant-Donor	No diagnostic abnormalities	Gunshot wound (Head)	33	M	Caucasian
L791D	1	Transplant-Donor	No diagnostic abnormalities	Anoxia (Cardiovascular)	53	M	Caucasian
L1129D	1	Transplant-Donor	No diagnostic abnormalities	Stroke (Intracranial Hemorrhage)	59	M	Caucasian
L1082D	1	Transplant-Donor	No diagnostic abnormalities	Head Trauma (Blunt Injury-Non MVA)	63	M	Caucasian
L367D	1	Transplant-Donor	No diagnostic abnormalities	Head trauma (Blunt injury)	80	M	Caucasian
L1560D	2	Transplant-Donor	Normal	Head Trauma- Blunt injury (MVA)	20	M	Caucasian
L935D	1	Transplant-Donor	No diagnostic abnormalities	Anoxia (Cardiovascular)	42	F	Caucasian
L1846D	1	Transplant-Donor	Normal	Cardiovascular - Anoxia	49	M	Caucasian
L1066D	1	Transplant-Donor	No diagnostic abnormalities	Stroke (Intracranial Hemorrhage)	57	F	Caucasian
L2236D	1	Donor	No diagnostic abnormalities	Anoxic brain injury due to hanging	40	M	Caucasian

Xenotech

Sample ID	Product #	Diagnosis	Macro fat %	Age	Gender	Ethnicity	BMI	Alcohol	Alcohol History	Diabetes
H0805	HHPL.NT	Normal	0	24	F	African American	54.6	No	NA	No
H0736	HHPL.NT	Normal	0	46	F	Caucasian	39.9	No	NA	Yes, NIDDM
H1275	HHPL.NT	Normal	0	47	F	African American	33.8	Yes	Heavy	No
H1293	HHPL.NT	Normal	0	52	F	Caucasian	29.1	No	NA	No
H0898	HHPL.NT	Normal	0	58	F	African American	31.3	No	NA	No
H0475	HHPL.NT	Normal	0	27	M	Caucasian	29.3	Yes	Heavy	No
H1271	HHPL.NT	Normal	0	30	M	African American	19.0	Yes	Moderate	No
H0402	HHPL.NT	Normal	0	32	M	Caucasian	25.7	Yes	Heavy	No
H0833	HHPL.NT	Normal	0	48	M	Hispanic	47.2	Yes	Social	Yes, NIDDM
H0944	HHPL.NT	Normal	1	49	M	Caucasian	41.8	Yes	Occasional	Yes, NIDDM

Supplemental Table 2. Normality tests of FcRn and β2M measured protein expressions.

	Anderson-Darling		D'Agostino & Pearson		Shapiro-Wilk		Kolmogorov-Smirnov	
	Pass	P value	Pass	P value	Pass	P value	Pass	P value
FcRn (n=39)	Yes	0.8935	Yes	0.8782	Yes	0.952	Yes	>0.1000
β2M (n=39)	No	0.0004	No	<0.0001	No	<0.0001	No	0.0162
β2M without outlier (n=38)	Yes	0.515	Yes	0.305	Yes	0.4804	Yes	>0.1000

Supplemental Figure 1. UPLC-MRM chromatograms of FcRn and β2M from L369D1 PNS. Three transitions of each peptide were monitored, and only IQVYSR for β2M and LFLEAFK for FcRn were detected and quantifiable.

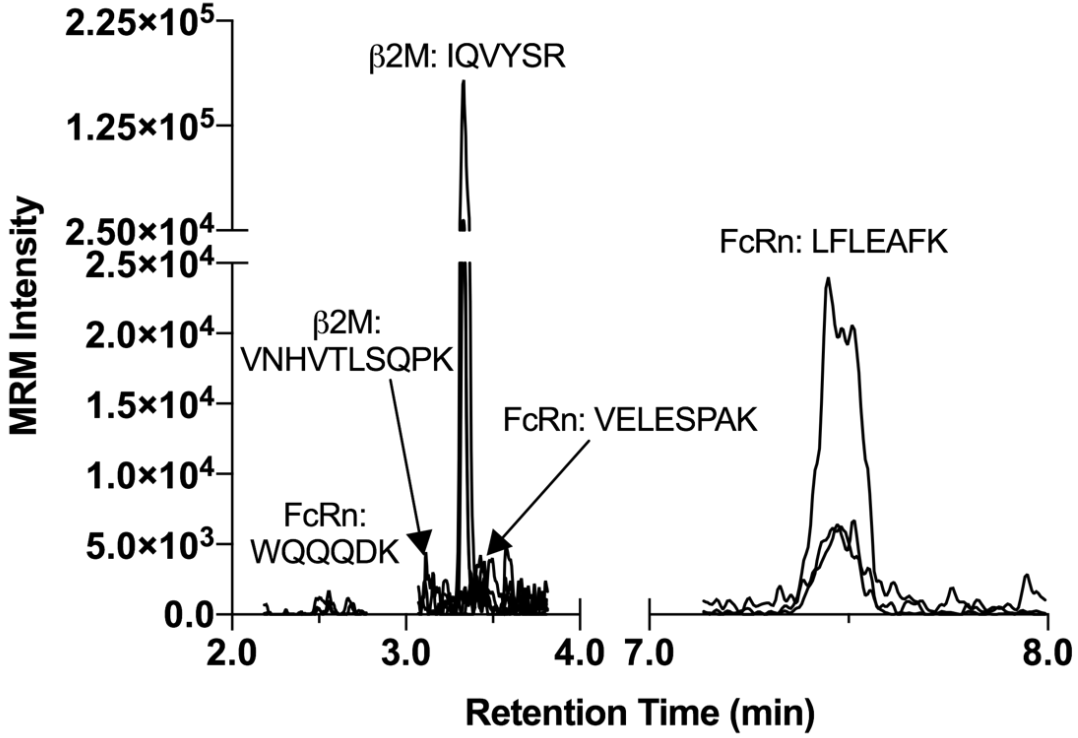

Supplemental Figure 2. Absolute quantification of FcRn (A) and β2M (B) for each individual liver tissue donor and concentration frequency distribution for FcRn (C) and β2M (D). Symbols and error bars in (A) and (B) represent the average and S. D. of triplicates of digestion for each human liver donor.

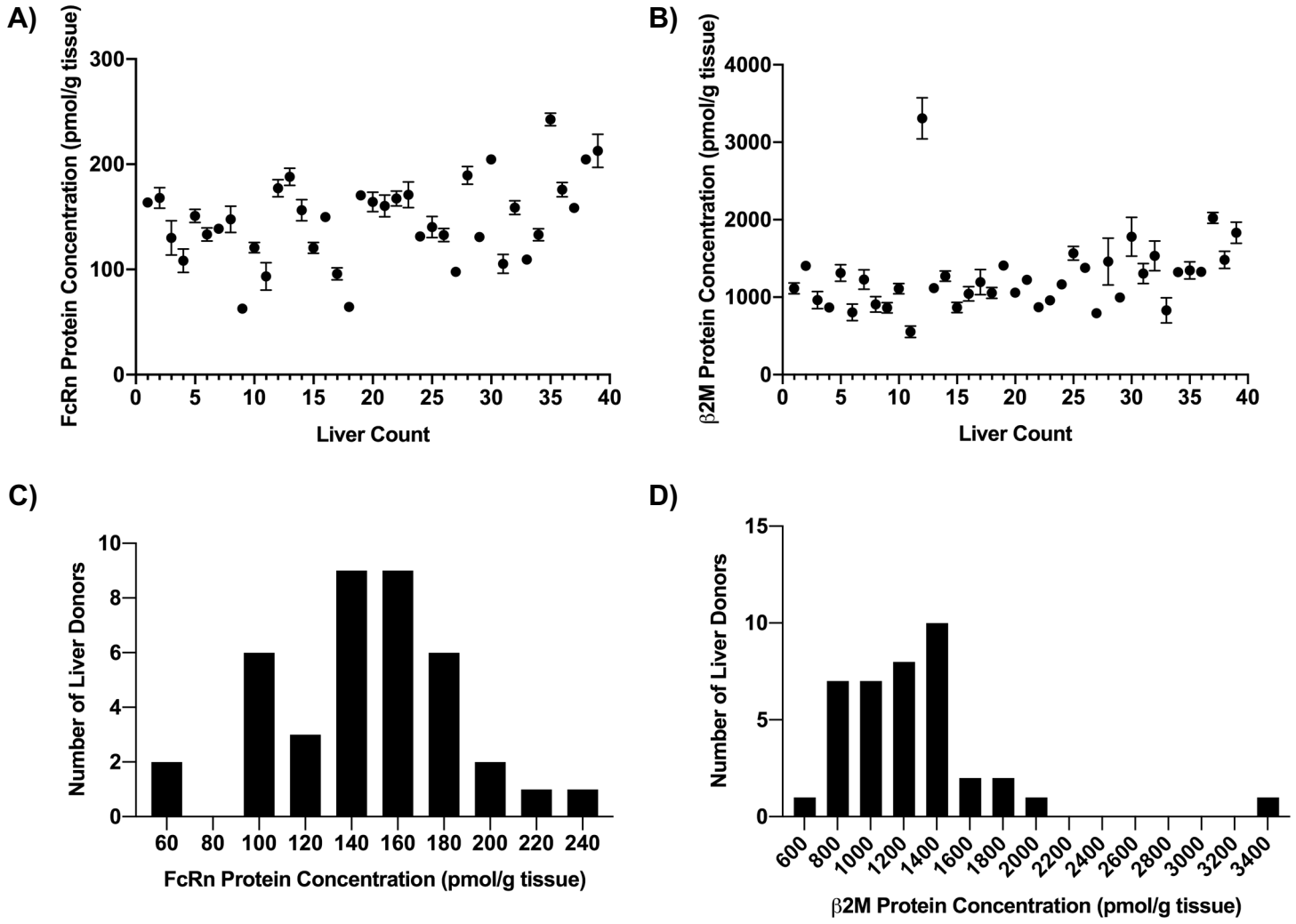

Supplemental Figure 3. β2M concentrations with outlier inclusion based on ethnicity. Lines and error bars represent the average and S. D. of all human liver analyzed in each ethnicity group. Symbols represent the average concentration determined from three separate digestions for each individual donor. Unpaired two-tailed t-test found no significant statistical differences between Caucasian and African American donors for β2M expressions excluding the statistical outlier determined by Grubb's test.

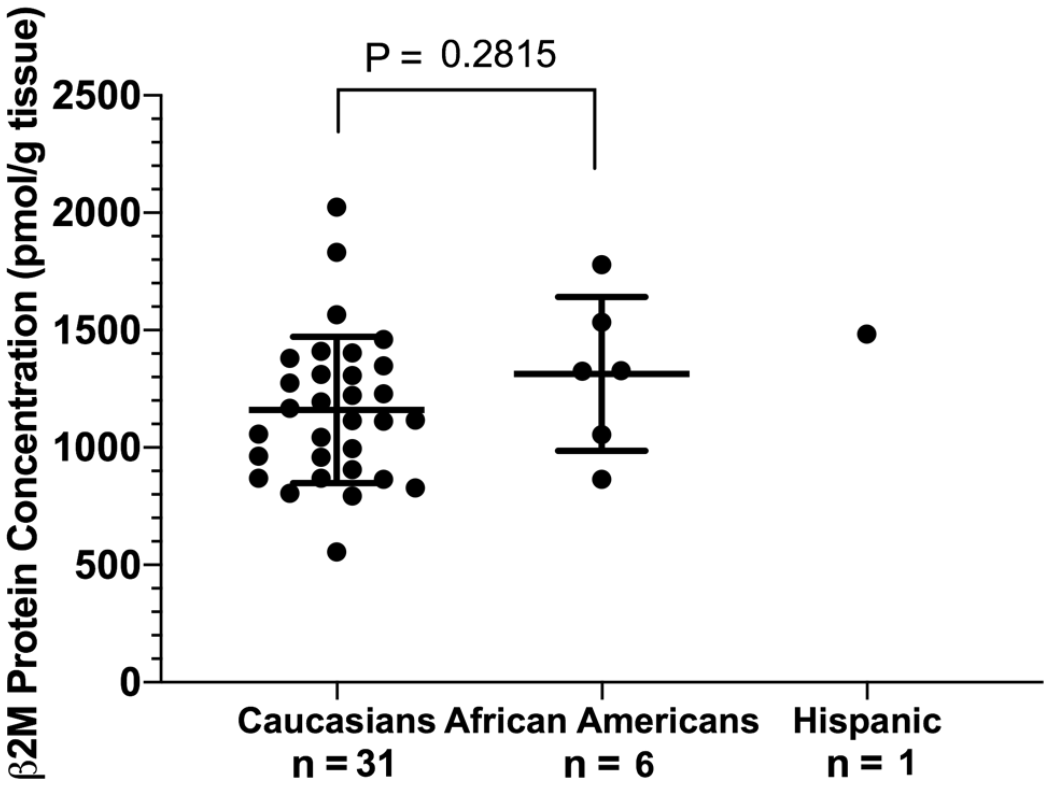

Supplemental Figure 4. Correlation analysis of FcRn concentration and β2M concentration without the outlier (n = 38). Symbols and error bars represent the average and S. D. of triplicates of digestion for each human liver donor. The dotted line represents the best-fit lines determined using least-square linear regression analysis.